Pseudo-Rabi oscillations in superconducting flux qubits in the classical regime

A. N. Omelyanchouk,[1] S. N. Shevchenko,[1] A. M. Zagoskin,[2,3,4] E. Il'ichev,[5] and Franco Nori[2,6]
[1]*B. Verkin Institute for Low Temperature Physics and Engineering, 61103, Kharkov, Ukraine*
[2]*Advanced Science Institute, RIKEN, Wako-shi, Saitama 351-0198, Japan*
[3]*Department of Physics and Astronomy, The University of British Columbia, Vancouver, British Columbia, Canada V6T 1Z1*
[4]*Department of Physics, Loughborough University, Leicestershire LE11 3TU, United Kingdom*
[5]*Institute of Photonic Technology (IPHT-Jena), P.O. Box 100239, D-07702 Jena, Germany*
[6]*Center for Theoretical Physics, Physics Department, Center for the Study of Complex Systems, The University of Michigan, Ann Arbor, Michigan 48109-1040, USA*
(Received 28 January 2008; published 15 August 2008)

Nonlinear effects in mesoscopic devices can have both quantum and classical origins. We show that a three-Josephson-junction (3JJ) flux qubit in the *classical* regime can produce low-frequency oscillations in the presence of an external field in resonance with the (high-frequency) harmonic mode ω of the system. Like in the case of *quantum* Rabi oscillations, the frequency of these pseudo-Rabi oscillations is much smaller than ω and scales approximately linearly with the amplitude of the external field. This classical effect can be reliably distinguished from its quantum counterpart because it can be produced by the external drive not only at the resonance frequency ω and its subharmonics (ω/n), but also at its overtones, $n\omega$.

DOI: 10.1103/PhysRevB.78.054512 PACS number(s): 74.50.+r, 03.67.Lx, 85.25.Cp

I. INTRODUCTION

The many advances in understanding the quantum behavior of mesoscopic and macroscopic systems over the last decade are due, to a large extent, to the investigation of superconducting qubits in the context of quantum computing.[1,2] These have led to the demonstration of their quantum behavior, at the level of one to four qubits.[3–6]

Since flux qubits can exhibit quantum superpositions of states differing by a macroscopic number of single-electron states, and the relevant observables can be accessed experimentally, these devices provide unique opportunities to investigate the *quantum-classical* frontier. Further scaling up of superconducting qubit networks (see, e.g., Ref. 7) is thus motivated by the needs of quantum information processing in solid state as well as by the fundamental interest in probing the limits of the applicability of quantum mechanics.

Once measurements are taken into account, the quantum behavior becomes fundamentally nonlinear. However, already at the classical level, nonlinearities are unavoidable in superconducting qubits, due to the essentially nonlinear behavior of Josephson junctions. It was recently pointed out that in a phase qubit, which is a biased single Josephson junction, the classical nonlinearity can produce effects with characteristics similar to Rabi oscillations[8] and Ramsey fringes,[9] which are often considered to be signatures of quantum behavior in two-level systems.

A. Rabi oscillations

In hindsight, pointing out Rabi oscillations in superconducting qubits as a decisive evidence of quantum behavior would be hard to justify, given the wealth of nonlinear classical effects in the Josephson systems. On the other hand, such statements should not be taken at face value, since the quantum behavior was in most cases established independently by other means.[2] The overemphasis on the quantum explanation and disinclination to invest additional effort in excluding a competing classical picture is understandable in such a fresh field, where the coherent behavior in large "artificial atoms" is only recently being observed on a regular basis.

The results in Refs. 8 and 9 raised the issue of the possible coexistence of similar nonlinear classical and quantum effects in-phase qubits. This issue has also been studied in Refs. 10 and 11. How to distinguish classical versus quantum behavior in superconducting qubits is an important question and the focus of this work.

Rabi oscillations (e.g., Ref. 12, p. 89) are coherent quantum transitions in a two-level system driven by an external ac field of amplitude A and with the characteristic frequency

$$\Omega = \sqrt{A^2 + (\delta\omega)^2}, \tag{1}$$

where $\delta\omega = |\omega - \omega_0|$ is its detuning from the interlevel distance, ω_0. In resonance, $\Omega = A$. This linear dependence on the field amplitude, and Ω being much less than other characteristic frequencies in the system, help identify Rabi oscillations. Indeed, they were observed in all types of superconducting qubits (see, e.g., Ref. 2). Multiphoton Rabi oscillations, at $\omega_0 = n\omega$, were also observed (see, e.g., Ref. 13).

In this paper we investigate a 3JJ flux qubit in the *classical* regime. With *two* independent variables instead of one, this is a richer system than the phase qubit of Ref. 8. We find that the resonant high-frequency driving ω produces low-frequency oscillations of the magnetic flux which are very similar to Rabi oscillations. We also show that a *qualitative* difference exists between these two effects, which allows to reliably distinguish them in experiments.

For a *phase* qubit, the possibility of experimental resolution between the classical and quantum behavior was recently investigated in Refs. 10 and 11. The distinction between classical and quantum oscillations is also an issue for very small mechanical oscillators. For example, Ref. 14 pro-

posed a spectroscopic approach to probe tiny vibrations of a nanomechanical resonator, which may reveal classical or quantum behavior depending on the decoherence-inducing environment. That proposal is based on the detection of the voltage-fluctuation spectrum in a superconducting transmission line resonator, which is indirectly coupled to the mechanical resonator via a controllable Josephson qubit acting as a quantum transducer. The classical (quantum mechanical) vibrations of the mechanical resonator induce symmetric (asymmetric) Stark shifts of the qubit levels, which can be measured by the voltage fluctuations in the transmission line resonator.[14] Thus, the motion of the mechanical resonator, including if it is quantum mechanical or not, could be probed by detecting the voltage-fluctuation spectrum of the transmission line resonator.

II. MODEL AND RESULTS

A. Flux qubit

Following Ref. 15, we consider a 3JJ flux qubit in the limit of negligible self-inductance $L \to 0$. The magnetic flux through the loop then equals the external applied flux Φ_e, and we introduce the reduced flux $\varphi_e = 2\pi\Phi_e/\Phi_0$. Here $\Phi_0 = h/2e$ is the flux quantum. Bistability is achieved due to the presence of three junctions in the loop. Due to the single valuedness of the superconducting wave function, one of the phase shifts across the Josephson junctions is eliminated through $\varphi_1 + \varphi_2 + \varphi_3 = \varphi_e$, leaving two independent variables: $\theta = (\varphi_1 + \varphi_2)/2$ and $\chi = (\varphi_1 - \varphi_2)/2$.

In the classical regime, the phase dynamics of the ith Josephson junction $(i = 1, 2, 3)$ can be described by the resistively shunted Josephson junction model,[16] in which the current is given by

$$I = \frac{\hbar C_i}{2e}\frac{d^2}{dt^2}\varphi_i + \frac{\hbar}{2eR_i}\frac{d}{dt}\varphi_i + I_{ci}\sin\varphi_i. \tag{2}$$

Here C_i is the junction capacitance, R_i its normal resistance, and I_{ci} its critical current. We now neglect the effect of thermal fluctuations, which are not crucial here. Following the common choice of parameters, we set $C_1 = C_2 = C$, $I_{c1} = I_{c2} = I_c$, $R_1 = R_2 = R$; $C_3 = \alpha C$, $I_{c3} = \alpha I_c$, $R_3 = R/\alpha$; $(0.5 \le \alpha \le 1)$. Introducing the dimensionless units, $\omega_0 t = \tau$,

$$\gamma = \frac{\hbar\omega_0}{2eRI_c} = \frac{\omega_0}{\omega_R}, \tag{3}$$

where

$$\omega_0 = \sqrt{\frac{2eI_c}{\hbar C}}, \quad \omega_R = \frac{2eRI_c}{\hbar}, \tag{4}$$

we can write the equations of motion for the variables θ, χ:

$$\frac{d^2}{d\tau^2}\chi + \gamma\frac{d}{d\tau}\chi = -\cos\theta\sin\chi,$$

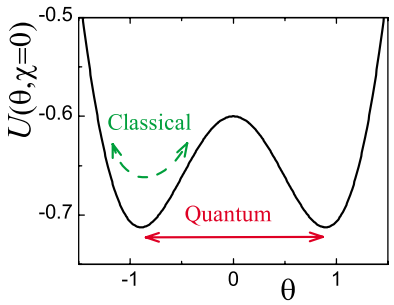

FIG. 1. (Color online) The potential profile of Eq. (9) with $\alpha = 0.8$, and $\varphi_e^d = \pi$. The arrows indicate *quantum* (solid line) and *classical* (dashed) oscillations.

$$(1+2\alpha)\frac{d^2}{d\tau^2}\theta + \gamma(1+2\alpha)\frac{d}{d\tau}\theta = -\sin\theta\cos\chi + \alpha\sin(\varphi_e - 2\theta) + \alpha\frac{d^2}{d\tau^2}\varphi_e + \alpha\gamma\frac{d}{d\tau}\varphi_e. \tag{5}$$

We consider the dc+ac reduced external flux

$$\varphi_e(t) \equiv 2\pi(\Phi_e/\Phi_0) = \varphi_e^d + \varphi_e^a\sin(\omega\tau). \tag{6}$$

The energy of the system is thus

$$H = E_J\left[\frac{1}{2}\left(\frac{d}{d\tau}\chi\right)^2 + \frac{1}{2}(1+2\alpha)\left(\frac{d}{d\tau}\theta\right)^2 - \cos\theta\cos\chi - \frac{1}{2}\alpha\cos(\varphi_e - 2\theta)\right], \tag{7}$$

where $E_J = \hbar I_c/2e$ is the Josephson energy. The canonical momenta are

$$p_\chi = E_J\frac{d\chi}{d\tau}, \quad p_\theta = E_J(1+2\alpha)\frac{d\theta}{d\tau}. \tag{8}$$

The effective potential is given by (Fig. 1)

$$U(\theta,\chi) = -\cos\theta\cos\chi - \alpha\cos(\varphi_e - 2\theta)/2. \tag{9}$$

If the dc static bias is $\varphi_e^d = \pi$, the system has degenerate minima at

$$\theta_0 = \pm\arccos[(2\alpha)^{-1}], \quad \chi_0 = 0.$$

The "plasma" frequencies of small oscillations around them are (in units of ω_0)

$$\omega_\theta = \sqrt{1-(2\alpha)^{-1}}, \quad \omega_\chi = (2\alpha)^{-1/2}.$$

B. Rabi-like classical oscillations

In the presence of the external field [Eq. (6)], the system will undergo forced oscillations around one of the equilibria. For $\alpha = 0.8$,[15] which is close to the parameters of the actual devices,[6,17,18] the values of the dimensionless frequencies become $\omega_\theta \approx 0.612$, and $\omega_\chi \approx 0.791$. Solving the equations of motion [Eq. (5)] numerically, we see the appearance of slow oscillations of the amplitude and energy superimposed on the

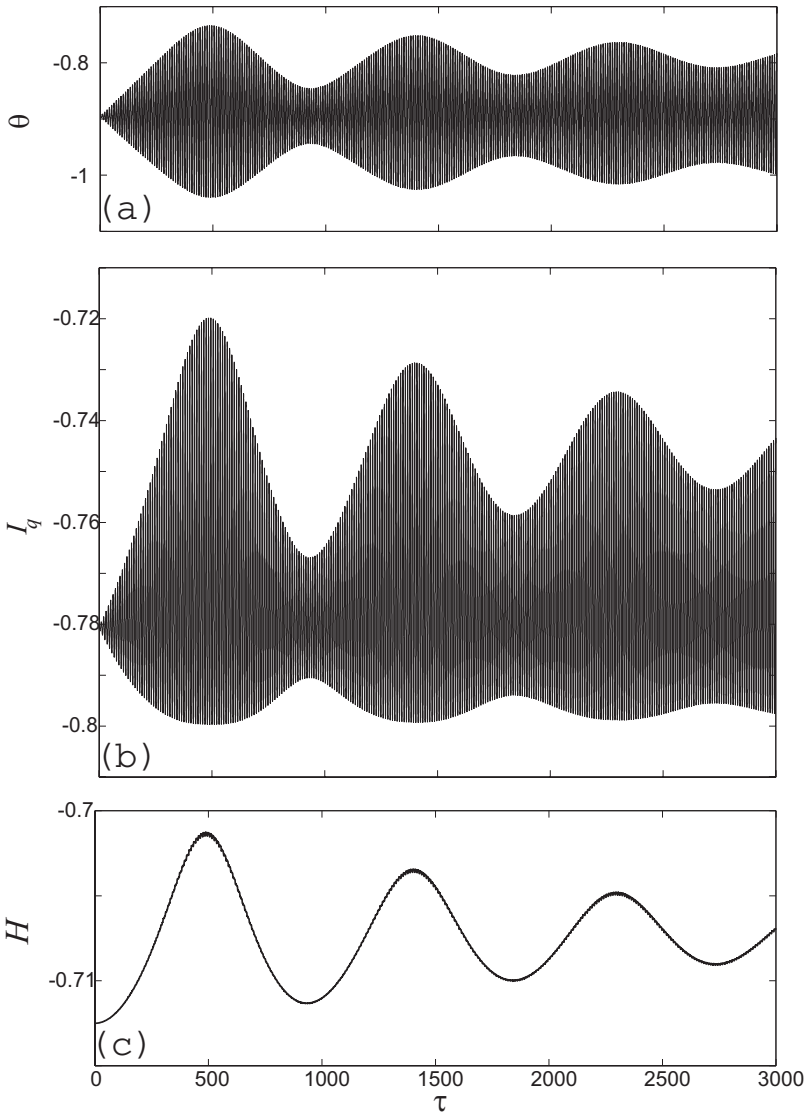

FIG. 2. (a) Driven oscillations around a minimum of the potential profile of Fig. 1 as a function of time. The driving amplitude is $\varphi_e^a=0.01$, driving frequency $\omega=0.612$, and the decay rate $\gamma=10^{-3}$. Low-frequency classical beat oscillations are clearly seen. (b) Low-frequency oscillations of the persistent current I_q in the 3JJ loop. (c) Same for the energy of the system.

fast forced oscillations (Fig. 2), similar to the classical oscillations in a phase qubit (Fig. 2 in Ref. 8) The dependence of the frequency of these oscillations on the driving amplitude shows an almost linear behavior in a wide range of frequencies around the resonance (Fig. 3), which justifies the "Pseudo-Rabi" moniker.

A quantitative difference between this effect and true Rabi oscillations is in the different scale of the resonance frequency. To induce Rabi oscillations (see, e.g., Ref. 19) between the lowest quantum levels in the potential (9), one must apply a signal in resonance with their tunneling splitting, which is exponentially smaller than ω_0. Still, this is not a very reliable signature of the effect, since the classical effect can also be excited by subharmonics, $\sim\omega_0/n$, as we can see in Fig. 4.

C. Observable ways to distinguish classical from quantum dynamics

The key observable difference between the classical and quantum cases, which would allow to reliably distinguish between them, is that the classical effect can also be produced by driving the system at the *overtones*, $\sim n\omega_0$, of the resonance signal (see Fig. 4). This effect can be detected using a standard technique for rf superconducting quantum interference devices (SQUIDs).[20] The current circulating in the qubit circuit produces a magnetic moment, which is measured by the inductively coupled high-quality tank circuit. For the tank voltage V_T we have

$$\frac{d^2V_T}{dt^2}+\frac{1}{\tau_T}\frac{dV_T}{dt}+\omega_T^2V_T=\omega_T^2M\frac{dI_q}{dt}, \tag{10}$$

where $\tau_T=R_TC_T$ is the RC constant of the tank, $\omega_T=(L_TC_T)^{-1/2}$ its resonant frequency, M the mutual inductance between the tank and the qubit, and $I_q(t)$ the current circulating in the qubit.

The persistent current in the 3JJ loop can be determined directly from Eq. (2). Its behavior in the presence of an external RF field is shown in Fig. 2(c). Note that the sign of the current does *not* change, which is due to the fact that the oscillations take place *inside* one potential well (dashed arrow in Fig. 1), and not *between* two separate nearby potential minima like in the quantum case. (Alternatively, this would

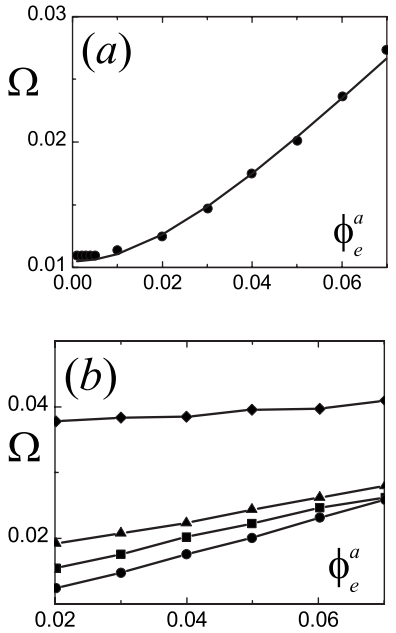

FIG. 3. (a) The dependence of the pseudo-Rabi frequency on the driving amplitude φ_e^a for $\omega=0.6$, $\gamma=10^{-3}$. The solid curve, $\Omega(\varphi_e^a)=0.35[(\varphi_e^a)^2+(\omega-0.63)^2]^{1/2}$, is the best fit to the calculated data. (b) The approximately linear frequency-amplitude dependence takes place in a wide region around the resonance: $\omega=0.6$ (circles), 0.625 (squares), 0.63 (triangles), 0.65 (diamonds).

also allow to distinguish between the classical and quantum effects by measuring the magnetization with a dc SQUID.)

There can be two strategies in detecting the slow oscillations, as long as the measurement time is smaller than their decay time, $\tau_R \sim 1/\gamma$, which is of order of the decay time of the qubit. First, one can directly measure the time-dependent voltage in the tank circuit, which from Eq. (10) is

$$V_T(\omega) = \frac{i\omega\omega_T^2 M}{\omega^2 - \omega_T^2 + i\omega/\tau_T} I_q(\omega). \tag{11}$$

Alternatively, one can measure the spectral density of the signal in the tank,

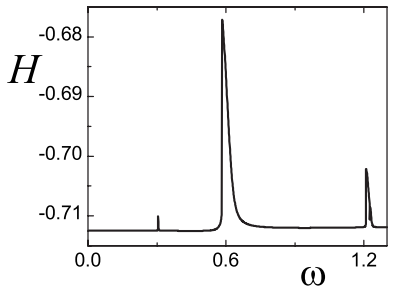

FIG. 4. The average energy H of the system as a function of the driving frequency ω. The main peak ($\omega_0 \approx 0.6$) corresponds to the resonance. The left peak at $\omega_0/2$ is the nonlinear effect of the excitation by a subharmonic, similar to a multiphoton process in the quantum case. The right peak at $2\omega_0$ is the first overtone and it has *no* quantum counterpart. Here $\varphi_e^d=\pi$; $\varphi_e^a=0.05$; $\gamma=10^{-3}$.

$$\langle V_T^2 \rangle_\omega = \frac{\omega^2 \omega_T^4 M^2}{(\omega^2 - \omega_T^2)^2 + \omega^2/\tau_T^2} \langle I_q^2 \rangle_\omega. \tag{12}$$

Choosing the tank frequency ω_T close to the classical low "Rabi" frequency Ω, in either case we use the tank as a filter, which removes the interference from the large, high-frequency driving field.

Generally, the magnitude of the observable voltage is proportional to the quality of the tank circuit, i.e., to τ_T. Nevertheless, τ_T must not exceed τ_R, otherwise the observed voltage oscillations, given by the solution to Eq. (10), will strongly depend on the (random) initial conditions, and no consistent picture will appear. On the other hand, after a time delay $\sim\tau_T$ the transients in the tank voltage die out, and this voltage becomes slaved to the qubit current. Therefore for the times $\tau_T < t < \tau_R$, while the Rabi oscillations of the qubit current persist, the effect (Rabi oscillations of the observed tank voltage) is directly observable. Under experimentally-accessible conditions, our calculated tank voltage amplitude exceeds 10 nV, which is measurable.

We find here an additional discriminant of the quantum versus classical behavior of the system. Indeed, in the quantum case, such a direct observation is impossible, due to the uncertainty principle, and the oscillations are only seen in the statistics of the measurements.

Remarkably, the effect on the correlators can be directly observed in both, the quantum and classical cases (in the quantum case such measurements are not limited by the decay time[18]). (Note also, that Eq. (12) is only valid for $\tau_T < t < \tau_R$, while the quantum noise can be observed indefinitely.)

III. CONCLUSIONS

In conclusion, we predict that a 3JJ flux qubit driven by a resonant external field will exhibit classical low-frequency oscillations superficially similar to the quantum Rabi oscillations in a driven two-level system. Both effects can coexist in the same region of parameters. A qualitative difference between the two (allowing to reliably distinguish between them) is that the classical effect can be also driven at the overtones of the resonant frequency.

ACKNOWLEDGMENTS

We acknowledge partial support from the National Security Agency (NSA), Laboratory for Physical Sciences (LPS), Army Research Office (ARO), National Science Foundation (NSF) Grant No. EIA-0130383, JSPS-RFBR 06-02-91200, MEXT Grant-in-Aid No. 18740224, JSPS-CTC program, the NSERC Discovery Grants Program (Canada), RSFQubit and EuroSQIP. S.N.S. acknowledges the financial support of INTAS under YS Grant No. 05-109-4479. A.N.O. and S.N.S. are grateful to Advanced Science Institute, RIKEN, for hospitality.

[1] J. Q. You and F. Nori, Phys. Today **58**(11), 42 (2005).
[2] G. Wendin and V. S. Shumeiko, in *Handbook of Theoretical and Computational Nanotechnology*, edited by M. Rieth and W. Schommers (American Scientific Publishers, Stevenson Ranch, California, 2006), Vol. 3, p. 223.
[3] Y. Nakamura, Y. A. Pashkin, and J. S. Tsai, Nature (London) **398**, 786 (1999).
[4] C. H. van der Wal, A. C. J. ter Haar, F. K. Wilhelm, R. N. Schouten, C. J. P. M. Harmans, T. P. Orlando, S. Lloyd, and J. E. Mooij, Science **290**, 773 (2000).
[5] A. Izmalkov, M. Grajcar, E. Il'ichev, T. Wagner, H. G. Meyer, A. Y. Smirnov, M. H. S. Amin, A. Maassen van den Brink, and A. M. Zagoskin, Phys. Rev. Lett. **93**, 037003 (2004); A. Izmalkov, M. Grajcar, S. H. W. van der Ploeg, U. Hübner, E. Il'ichev, H.-G. Meyer, and A. M. Zagoskin, Europhys. Lett. **76**, 533 (2006).
[6] M. Grajcar *et al.*, Phys. Rev. Lett. **96**, 047006 (2006).
[7] J. Q. You, Y. Nakamura, and F. Nori, Phys. Rev. B **71**, 024532 (2005); Y. X. Liu, L. F. Wei, J. S. Tsai, and F. Nori, Phys. Rev. Lett. **96**, 067003 (2006); M. Grajcar, Y. X. Liu, F. Nori, and A. M. Zagoskin, Phys. Rev. B **74**, 172505 (2006); S. Ashhab, S. Matsuo, N. Hatakenaka, and F. Nori, *ibid.* **74**, 184504 (2006); Y. X. Liu, L. F. Wei, J. R. Johansson, J. S. Tsai, and F. Nori, *ibid.* **76**, 144518 (2007).
[8] N. Gronbech-Jensen and M. Cirillo, Phys. Rev. Lett. **95**, 067001 (2005).
[9] J. E. Marchese, M. Cirillo, and N. Gronbech-Jensen, Open Syst. Inf. Dyn. **14**, 189 (2007).
[10] J. Lisenfeld, A. Lukashenko, M. Ansmann, J. M. Martinis, and A. V. Ustinov, Phys. Rev. Lett. **99**, 170504 (2007).
[11] S. N. Shevchenko, A. N. Omelyanchouk, A. M. Zagoskin, S. Savel'ev, and F. Nori, New J. Phys. **10**, 073026 (2008).
[12] P. Meystre and M. Sargent III, *Elements of Quantum Optics*, 2nd ed. (Springer-Verlag, Berlin, 1991).
[13] S. Saito, T. Meno, M. Ueda, H. Tanaka, K. Semba, and H. Takayanagi, Phys. Rev. Lett. **96**, 107001 (2005); V. I. Shnyrkov, Th. Wagner, D. Born, S. N. Shevchenko, W. Krech, A. N. Omelyanchouk, E. Il'ichev, and H.-G. Meyer, Phys. Rev. B **73**, 024506 (2006).
[14] L. F. Wei, Y. X. Liu, C. P. Sun, and F. Nori, Phys. Rev. Lett. **97**, 237201 (2006).
[15] J. E. Mooij, T. P. Orlando, L. Levitov, L. Tian, C. H. van der Wal, and S. Lloyd, Science **285**, 1036 (1999).
[16] A. Barone and G. Paterno, *Physics and Applications of the Josephson Effect* (Wiley, New York, 1982).
[17] I. Chiorescu, Y. Nakamura, C. Harmans, and J. Mooij, Science **299**, 1869 (2003).
[18] E. Il'ichev, N. Oukhanski, A. Izmalkov, Th. Wagner, M. Grajcar, H.-G. Meyer, A. Smirnov, A. Maassen van den Brink, M. H. S. Amin, and A. Zagoskin, Phys. Rev. Lett. **91**, 097906 (2003).
[19] S. Ashhab, J. R. Johansson, and F. Nori, New J. Phys. **8**, 103 (2006); S. Ashhab, J. R. Johansson, A. Zagoskin, and F. Nori, Phys. Rev. A **75**, 063414 (2007); S. N. Shevchenko, A. S. Kiyko, A. N. Omelyanchouk, and W. Krech, Low Temp. Phys. **31**, 569 (2005).
[20] A. Golubov, M. Kupriyanov, and E. Il'ichev, Rev. Mod. Phys. **76**, 411 (2004).